Environmental Science & Technology

Article

pubs.acs.org/est

Molecular Simulations of Carbon Dioxide and Water: Cation Solvation

Louise J. Criscenti* and Randall T. Cygan

Geochemistry Department, P.O. Box 5800 MS 0754, Sandia National Laboratories, Albuquerque, New Mexico 87185-0754, United States

ABSTRACT: Proposed carbon dioxide sequestration scenarios in sedimentary reservoirs require investigation into the interactions between supercritical carbon dioxide, brines, and the mineral phases found in the basin and overlying caprock. Molecular simulations can help to understand the partitioning of metal cations between aqueous solutions and supercritical carbon dioxide where limited experimental data exist. In this effort, we used classical molecular dynamics simulations to compare the solvation of alkali and alkaline-earth metal cations in water and liquid CO_2 at 300 K by combining a flexible simple point charge model for water and an accurate flexible force field for CO_2. Solvation energies for these cations are larger in water than in carbon dioxide, suggesting that they will partition preferentially into water. In both aqueous and CO_2 solutions, the solvation energies decrease with cation size and increase with cation charge. However, changes in solvation energy with ionic radii are smaller in CO_2 than in water suggesting that the partitioning of cations into CO_2 will increase with ion size. Simulations of the interface between aqueous solution and supercritical CO_2 support this suggestion in that some large cations (e.g., Cs^+ and K^+) partition into the CO_2 phase, often with a partial solvation sphere of water molecules.

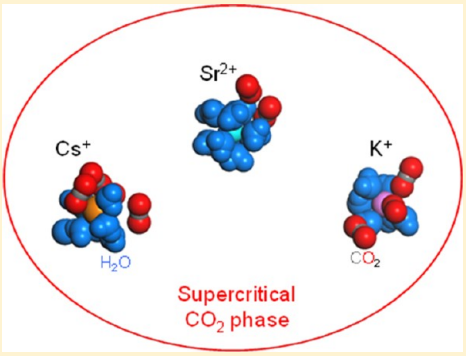

INTRODUCTION

To develop accurate regional scale models to evaluate the fate of supercritical CO_2 in various CO_2 sequestration scenarios, it is important to assess the exchange of solutes across the supercritical CO_2–water interface. Experimental studies[1−7] of the solubility of CO_2 in water and simple aqueous solutions have been used to determine the range of CO_2 concentrations trapped in idealized reservoir fluids in regional scale multiphase models. However, the interaction of supercritical CO_2 with the complex brine compositions found in aquifers have typically been ignored in such hydrological simulations, most likely because of the lack of data (solubility, density, partition coefficients, etc.) for these interactions at the temperatures and pressures expected in geological reservoirs. Recent experimental and simulation studies[8−12] of the geochemistry of reservoir fluids and mineral interactions have provided new insights on supercritical CO_2 behavior in geological media. Rempel et al.[13] present experimental data for the fractionation of Na, Fe, Cu, and Zn between brine and CO_2 for pressures of 6.6−16 MPa at 340 K. The data exhibit an increase in Na concentrations with increasing CO_2 density and suggest that Fe, Cu, and Zn could be transferred to adjacent aquifer systems. However, this experimental approach is recently developed and difficult to implement. Therefore, geochemical modeling of reactions among reservoir rocks, brine, and supercritical CO_2 focus on investigating the impact of high PCO_2 on reactions between saline brines and minerals under reservoir conditions, but, as a first approximation, neglect the solubility of water, salts, or metals in the supercritical phase.[14]

Because of limited experimental data on metal partitioning between supercritical CO_2 and brine solutions, it is valuable to consider the use of computational chemistry methods to explore this subject. Metal partitioning into the supercritical CO_2 phase may influence chemical reactions such as the dissolution of primary phases or precipitation of secondary minerals, and physical properties such as both the density and viscosity of the CO_2 phase, and the contact angles formed between supercritical CO_2, water, and mineral phases. Supercritical CO_2 has been considered as a potential fluid for extracting metal ions from liquid phases. The ions cannot readily be extracted in supercritical CO_2, but the use of metal–organic complexes greatly increases metal partitioning into the supercritical phase.[15] This suggests that metal speciation in the brine may also impact species partitioning between the two fluids.

The research presented here provides a first look at the solvation of alkali and alkaline-earth metal cations in CO_2 fluids and the likelihood that these cations will partition between brines and supercritical CO_2 in sedimentary basin environments. An overall goal of our research is to use molecular simulations to model the structure and behavior of injected supercritical CO_2 in subsurface reservoirs and how it eventually

Special Issue: Carbon Sequestration

Received: April 23, 2012
Revised: July 6, 2012
Accepted: July 10, 2012
Published: July 10, 2012

interacts with resident aqueous fluids and minerals over time. In the present study we use molecular dynamics to investigate the structure of the CO_2–brine interface and how electrolytes, specifically alkali and alkaline earth cations, are partitioned between aqueous and CO_2 phases. We report the application of an accurate and flexible CO_2 force field, compare cation solvation in water and CO_2 systems, and examine the solubility of CO_2 in water.

COMPUTATIONAL METHODS

Carbon Dioxide Force Field. For the molecular simulations of this study, we use the fully flexible CO_2 force field developed by Cygan et al.[16] The three-point force field uses the refined Van der Waals parameters of Zhu et al.[17] that were derived from the original model of Harris and Young.[18] The force field also allows for full intramolecular bond stretch and angle bend and thus correctly predicts the vibrational spectra of CO_2. The CO_2 potential is compatible with most point-charge force fields including Clayff[19] and other related force fields for the simulation of geochemical systems. The interatomic potentials should be appropriate for simulating complex CO_2 systems involving multiple phases, interfaces, and the addition of dissolved cations in both water and CO_2 phases.

In the Cygan et al.[16] force field, the total potential energy of the molecular system is described by Coulombic and van der Waals contributions representing nonbonded energies and bond-stretch and angle-bend terms representing the intramolecular energies. The long-range Coulombic or electrostatic energy is given by eq 1, where q_i and q_j are the partial charges of the atoms and r_{ij} is the distance between the atoms.

$$E_{Coul} = \frac{q_i q_j}{r_{ij}} \tag{1}$$

The short-range van der Waals energy is given by

$$E_{VDW} = 4\varepsilon_{ij}\left[\left(\frac{\sigma_{ij}}{r_{ij}}\right)^{12} - \left(\frac{\sigma_{ij}}{r_{ij}}\right)^{6}\right] \tag{2}$$

where ε_{ij} and σ_{ij} are optimized for intermolecular interactions using values determined by Zhu et al.[17] The interaction parameters between unlike atoms are calculated according to the arithmetic mean rule for the distance parameter, σ_{ij}, and the geometric mean rule for the energy parameter, ε_{ij}.[20,21] Harmonic potentials are used for the bond stretch and angle bend terms.

$$E_{Stretch} = \frac{1}{2}k_S(r_{ij} - r_o)^2 \tag{3}$$

$$E_{Bend} = \frac{1}{2}k_B(\theta_{ijk} - \theta_o)^2 \tag{4}$$

Both expressions describe the increase in the potential energy based on force constants k_S and k_B and the deviations from the equilibrium geometry (r_o and θ_o) of the CO_2 molecules. The potential energy for any configuration of CO_2 molecules in a periodic simulation cell is evaluated using this set of potentials by summing all possible pairwise interactions. Ewald summation is used to ensure convergence of the long-range Coulombic energy. van der Waals contributions are calculated using a cubic spline with a 12.5 Å cutoff. The Coulombic and van der Waals contributions are excluded when evaluating intramolecular interactions.

Molecular Dynamics Simulations. Classical molecular dynamics (MD) was used to evaluate the structure and thermodynamics of the solvation of alkali and alkaline earth cations by CO_2, and to examine the structure of the water–CO_2 interfaces. The Forcite software[22] was used to evaluate the electrostatic and short-range interactions for each atomic configuration and time step. MD simulations were performed using a canonical *NVT* thermodynamic ensemble, maintaining a fixed cell volume for a fixed number of atoms. Temperature was controlled using the Nose–Hoover[23] method. One million time steps of 1 fs were used to obtain 1 ns of simulation time; atomic configurations were saved every 1000 time steps (1 ps) for efficient data storage and trajectory analysis. MD simulations of systems involving water–CO_2 and brine–CO_2 interfaces were completed for 0.5 ns of simulation time using the same frequency of molecular configuration storage.

Cation Solvation in Liquid Carbon Dioxide. MD simulations of alkali and alkaline earth cation solvation in liquid CO_2 were performed using the *NVT* thermodynamic ensemble with 512 CO_2 molecules in a simulation box (V = 48.23 nm^3; ρ = 0.77 g/cm^3 at 8 MPa) at 300 K for comparison with cation solvation in liquid water which is typically determined at ambient temperature and pressure (300 K, 0.1 MPa).[24,25] A simulation was performed for 1 ns to equilibrate the liquid CO_2 in a cubic periodic cell with a cell length of 36.4 Å. Subsequently, each cation was placed in the equilibrated model CO_2 liquid. A similar set of simulations was completed for the same number of CO_2 molecules at supercritical conditions (350 K, 20 MPa) using a cubic periodic cell with a cell length of 39.2 Å (V = 60.24 nm^3; ρ = 0.62 g/cm^3). For both conditions, each solvation model was initially geometry-optimized for 500 iterations prior to 1 ns of MD simulation. Charge balance was established by using a charge-neutralizing background.[20,26] The solvation energy for a particular cation was estimated by subtracting the potential energy of the equilibrated liquid CO_2 simulation cell from the potential energy of the equilibrated simulation cell containing liquid CO_2 (or supercritical CO_2) and the cation [i.e., PE(CO_2 + cation) − PE(CO_2 cell)]. The van der Waals parameters used for the alkali (Li^+, Na^+, K^+, and Cs^+) and alkaline earth cations (Mg^{2+}, Ca^{2+}, Sr^{2+}, Ba^{2+}) are provided in Table 1. Four cations of each series were studied to establish trends in solvation energy with cation size. The van der Waals parameters were all determined from calculations performed to describe cation–water interactions. Therefore, as a first-order approximation, we assume the intrinsic parameters used for each cation from calculations in aqueous solutions are the same for the CO_2 solutions when combined with the CO_2 parameters. The calculated solvation energies for the alkali and alkaline earth metals in CO_2 were

Table 1. Force Field Parameters for Cations

cation[a]	ε_i (kJ/mol)	σ_i (Å)
Li^+ [40]	0.0766	1.3723
Na^+ [25]	0.5447	2.3500
K^+ [41]	0.4187	3.3340
Cs^+ [42]	0.4187	3.8310
Mg^{2+} [40]	3.6634	1.6444
Ca^{2+} [41]	0.4187	2.8720
Sr^{2+} [40]	0.4187	3.4620
Ba^{2+} [40]	0.1968	3.8166

[a]Smith and Dang,[25] Koneshan et al.,[41] Smith and Dang,[42] Åqvist[40].

dx.doi.org/10.1021/es301608c | Environ. Sci. Technol. 2013, 47, 87–94

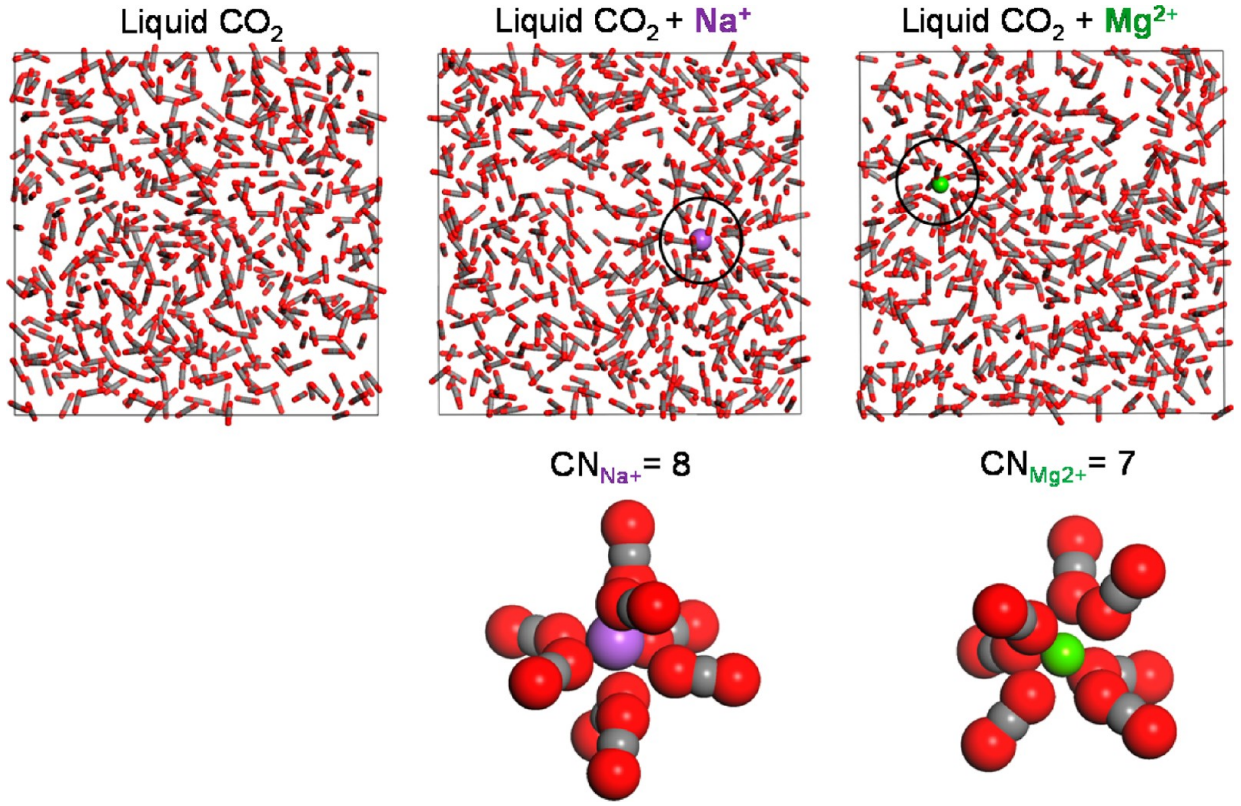

Figure 1. Equilibrated cells of liquid CO_2, and Na^+ and Mg^{2+} solvated in liquid CO_2 from MD simulations at 300 K after 1 ns of simulation time. Details of CO_2 coordination spheres about cations are presented below the respective simulation cells.

compared to the enthalpies of solvation for these cations in H_2O provided by Franks.[24]

Models of the Water–Supercritical Carbon Dioxide Interface. Molecular dynamics simulations of water–supercritical CO_2 interface were completed using *NVT* ensemble, 6912 H_2O molecules, 2048 CO_2 molecules, and appropriate densities at 20 MPa and 350 K (0.98 g/cm^3 for H_2O and 0.62 g/cm^3 for supercritical CO_2). Carbon dioxide is modeled using the Cygan et al.[16] flexible potential described earlier. Water is represented by the simple point charge (SPC) water model[27] combined with harmonic bond stretching and angle bending based on the intramolecular parameters from Teleman et al.[28] We use a three-dimensional periodic simulation cell (74.5 Å × 74.5 Å × 78.0 Å) in which the interface between the two phases is allowed to evolve for 0.5 ns—sufficient to obtain local equilibrium and to monitor the evolution of the interfacial region. A vacuum gap of approximately 1.5–2.5 Å was constructed between the two phases at the interfaces to avoid any initial high energy environment. Effectively, the simulation cell incorporates lamellae of water and CO_2 regions with two interfaces, one in the central region of the cell which we monitor, and another on the cell side boundary which is ignored.

A periodic simulation cell similar to that used for the water–supercritical CO_2 interface was constructed to demonstrate the partitioning of various alkali and alkaline earth cations between the two phases at 20 MPa and 350 K. The initial configuration incorporated the water–CO_2 interface with a uniform distribution of seven cations (Na^+, K^+, Cs^+, Mg^{2+}, Ca^{2+}, Sr^{2+}, and Ba^{2+}) at the central interface. Four of each cation type were placed at the interface with no two cations within 9 Å of each other. This arrangement corresponds to an approximate total concentration of 0.1 M assuming equal solvent molecule contributions. Particular care in the initial configuration of cations at the interface ensures minimal bias in solvent molecule preference. No counteranions are included in the simulation cell so as to limit ion–ion associations and avoid biasing the partitioning between phases. Charge balance is achieved by a neutralizing background of approximately −0.0001 e/Å^3 which is relatively small and is expected to have minimal impact on the cation distributions. Nonetheless, this constraint would necessarily be relaxed by the inclusion of explicit counterions in a more realistic simulation.[29,30] As with the MD simulation of the pure water–supercritical CO_2 interface, we allow the system to evolve for 0.5 ns while saving configurations every 1000 time steps (1 ps).

RESULTS AND DISCUSSION

Cation Solvation Structure. The cations are solvated in liquid CO_2, with a clearly defined first solvation shell. Figure 1 illustrates an equilibrated simulation cell of liquid CO_2 and corresponding equilibrated simulation cells for a single Na^+ and a single Mg^{2+} cation in liquid CO_2. It can clearly be seen that the structure of liquid CO_2 is disrupted by the presence of the cations and that the CO_2 molecules orient around both Na^+ and Mg^{2+} such that one oxygen atom of each coordinating molecule is immediately associated with the cation. Details of the CO_2 coordination spheres are provided below the respective simulation cells. The comparative sizes of the Na^+ and Mg^{2+} cations are based on their relative ionic radii.

In the top half of Figure 2, a comparison between the structure of simulated liquid CO_2 (300 K, ρ = 0.77 g/cm^3 at 8 MPa) and supercritical CO_2 (350 K, p = 0.62 g/cm^3 at 20 MPa) is provided through radial distribution functions (RDFs)

dx.doi.org/10.1021/es301608c | *Environ. Sci. Technol.* 2013, 47, 87–94

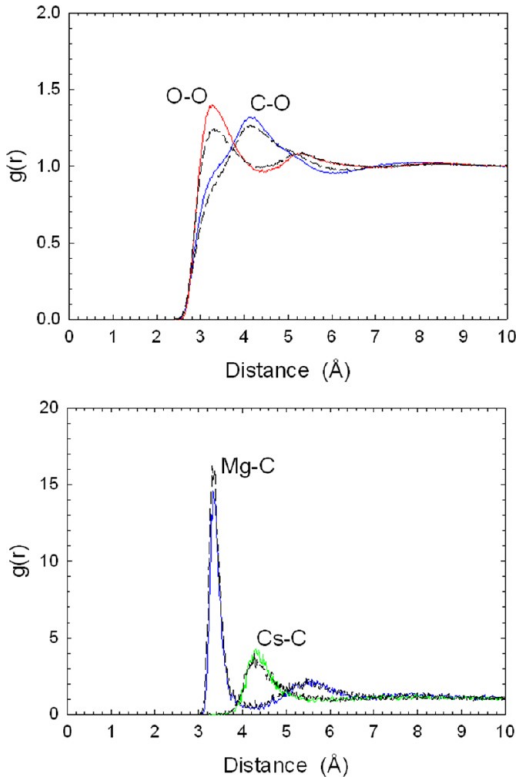

Figure 2. (top) Radial distribution functions for pure liquid CO_2 (solid line) and supercritical CO_2 (dash line); (bottom) radial distribution functions for Mg^{2+} and Cs^+ cations solvated by liquid CO_2 (solid line) and supercritical CO_2 (dash line). RDFs derived from equilibrium MD trajectories obtained at 300 K and 8 MPa for liquid CO_2 and 350 K and 20 MPa for supercritical CO_2.

for the intermolecular O−O and C−O distances. The difference in the local structure between the two fluids that we simulated is not large as demonstrated by a slight shift in the primary O−O peak position at 3.2 Å. Broader O−O peaks occur at approximately 5.2 Å and relate to some structure in the second coordination sphere of CO_2 molecules. The C−O peaks centered at 4.2 Å include a shoulder at about 3.2 Å representing a closer contact between CO_2 molecules, most likely associated with a T-shaped molecular configuration.[31] In the bottom half of Figure 2, the RDFs for a small divalent cation (Mg^{2+}) and a large monovalent cation (Cs^+) in both liquid CO_2 and supercritical CO_2 are illustrated. The RDFs for Mg^{2+} exhibit relatively sharp first-coordination peaks at 3.3 Å and broad second peaks at 5.5 Å. The Cs^+ RDFs only display the first coordination peak (4.3 Å) and are less structured compared to those for Mg^{2+}, which is consistent with the difference in CO_2 solvation energies for the two cations (see below). The RDF curves derived for liquid and supercritical solvents exhibit some overlap for each cation, suggesting that the solvation of alkali and alkaline earth cations is similar in CO_2 under both conditions. We observe similar comparisons between the RDFs for liquid and supercritical CO_2 solvation of intermediate-sized cations (not shown).

The number of CO_2 molecules in the first solvation shell around each cation was determined from RDFs such as those depicted in the bottom graph of Figure 2. The first peak maximum represents the average cation−C distance and the first peak minimum is characteristic of the outer radius of the first solvation shell. In general, for both suites of metal cations, the cation−C distance increases as a function of cation size. Comparison of the RDFs for the alkali metals and the alkaline earth metals suggests that the divalent metals impose more structure on the solvent. This is illustrated in Figure 2: the first peak of the Mg−C RDF has a higher intensity than the Cs−C peak, and the Mg−C RDF exhibits a clearly defined second maximum and minimum suggesting the presence of a second well-structured solvation shell.

Integration of the RDFs for the cation−carbon distances provides the number of coordinating CO_2 molecules about each cation. The cutoff for the first solvation shell is usually correlated with the first minimum in the RDF curves. From Figure 2, it can be seen that the trough between the peaks in the Mg RDF is relatively flat over a 0.25 Å distance, allowing for some discretion in determining the upper limit of integration which can result in a variation of one molecule in the first solvation shell. The coordination number varies primarily with cation size. For the alkali metals, the coordination numbers are 4−5 for Li^+, 6 for Na^+, 8 for K^+, and 9 for Cs^+. For the alkaline earth metals, the coordination numbers are 6−7 for Mg^{2+}, 8−9 for Ca^{2+}, 10 for Sr^{2+}, and 10−11 for Ba^{2+}.

Overall, the coordination numbers for cations in water tend to be somewhat smaller. Reported experimental coordination or hydration numbers for cations differ depending on the method of analysis. However, in general, the numbers reported from experiment for the alkali metals are 4 for Li^+, 6 for Na^+, and 6−8 for both K^+ and Cs^+.[32] For the alkaline earth metals, the coordination numbers determined experimentally are 6 for Mg^{2+},[32] 7−8 for Ca^{2+},[33−35] 6−10 for Sr^{2+},[36,37] and 9.5 for Ba^{2+}.[32] These experimentally determined numbers compare well to those determined from molecular dynamics simulations in a previous study: 6 for Mg^{2+}, 6−7 for Ca^{2+}, 8 for Sr^{2+}, 8.8 for Ba^{2+}.[38] The higher coordination numbers observed for CO_2 solvent than those for water are likely due to steric considerations associated with the ability to align more linear CO_2 molecules than angular H_2O molecules about the sphere of a closed-shell cation.

Cation Solvation Thermodynamics. A comparison between the solvation energies for the various alkali and alkaline earth cations obtained by MD simulation (solvated by liquid CO_2) and the solvation enthalpies for the cations in water reported in the literature[24] is provided in Figure 3. In all cases, the solvation energies for the cations in water are larger (i.e., more negative), indicating that the cations prefer to be solvated in water than in carbon dioxide. However, the differences in solvation energies for the alkali metals in the two solvents is relatively small (<40 kcal/mol) compared to the differences observed for the alkaline earth metals (>135 kcal/mol). In addition, for both series of cations, changes in solvation energy with increasing ionic radii are smaller in CO_2 than in water, suggesting that the overall partitioning of cations into CO_2 will increase with ion size. In all cases, the cations prefer solvation by H_2O, with the most likely cations to partition into CO_2 to be those with nearly equal solvation energies in both fluids, namely K^+ and Cs^+.

Solvation energies derived from the MD simulations for cations by supercritical CO_2 follow trends in cation size similar to those observed for liquid CO_2 but with a decrease in solvation energy (less negative values) by approximately 50 kcal/mol. However, potential energies obtained for the equilibrium configurations exhibit relatively large variation (25−30%) at supercritical conditions and ultimately result in large uncertainties in the calculated solvation energy. We also

dx.doi.org/10.1021/es301608c | Environ. Sci. Technol. 2013, 47, 87−94

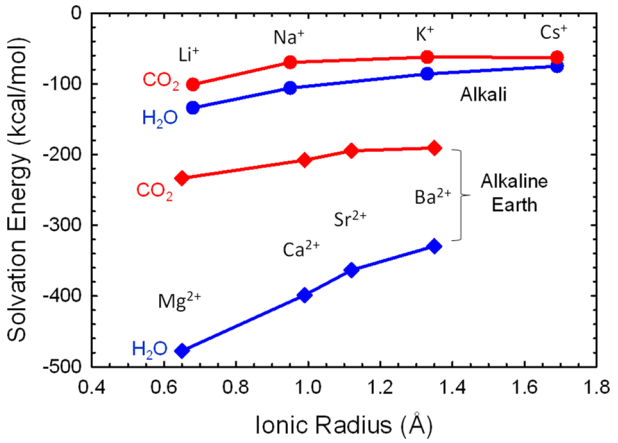

Figure 3. Comparison of solvation energies for various alkali and alkaline earth cations obtained by MD simulation (solvated by liquid CO_2 at 300 K) and from experiment (solvated by H_2O at 300 K) as a function of cation ionic radius; uncertainties in the solvation energies are less than the symbol size.

examined the change in volume associated with the solvation of Cs^+ by liquid CO_2 and its effect on the calculated solvation energy. For this extreme case—Cs^+ is the largest cation and has the lowest solvation energy—we compare the solvation energy obtained for a simulation cell having an expanded volume associated with the Cs^+–CO_2 coordination sphere (200 $Å^3$) with that derived for the original solvation cell. The resulting solvation energy for the expanded cell is statistically equivalent, well within the estimated 5% relative uncertainty we obtain for the original simulation cell.

Water–Supercritical Carbon Dioxide Interface. Molecular dynamics simulations of the water–supercritical CO_2 interface provide insights into the dynamical evolution of relatively immiscible fluids in addition to testing the suitability of combining interaction potentials for the two fluids. Figure 4 includes snapshots of both the initial configuration and the resulting structure of the water–supercritical CO_2 interface after 0.5 ns of simulation, and the corresponding compositional profile across the central interface. Using standard combination rules[21] for the van der Waals interactions between water and CO_2 our MD results clearly exhibit a diffuse and stable interface between the two phases. Additionally, a significant number of CO_2 molecules have diffused from the bulk CO_2 into the water region to form a homogeneous distribution of dissolved CO_2 in water at a concentration of about 0.02 mole fraction. This predicted concentration represents the limiting solubility of CO_2 in water and is similar to the experimental value[1] for the modeled conditions, considering that the classical simulation does not allow for dissociation or reaction of the classical CO_2 model into bicarbonate or other carbonate species. In contrast to the dissolution of CO_2 into water, the MD simulation exhibits only a trace amount of water molecules in the supercritical CO_2 phase consistent with the expected insolubility of water. The resulting compositional profiles for both components clearly exhibit a diffuse transitional region of about 10 Å defining the molecular interface between the phases. Recently, Vlcek et al.[39] have used heteroatomic van der Waals parameters to improve the accuracy of standard H_2O and CO_2 potentials in the prediction of mutual solubilities and tracer diffusion coefficients.

Cations and the Supercritical Water–Carbon Dioxide Interface. Given the comparison of solvation energies of various alkali and alkaline earth cations derived from MD simulations and the dependence of partitioning on cation charge and size, it is helpful to demonstrate the likely behavior

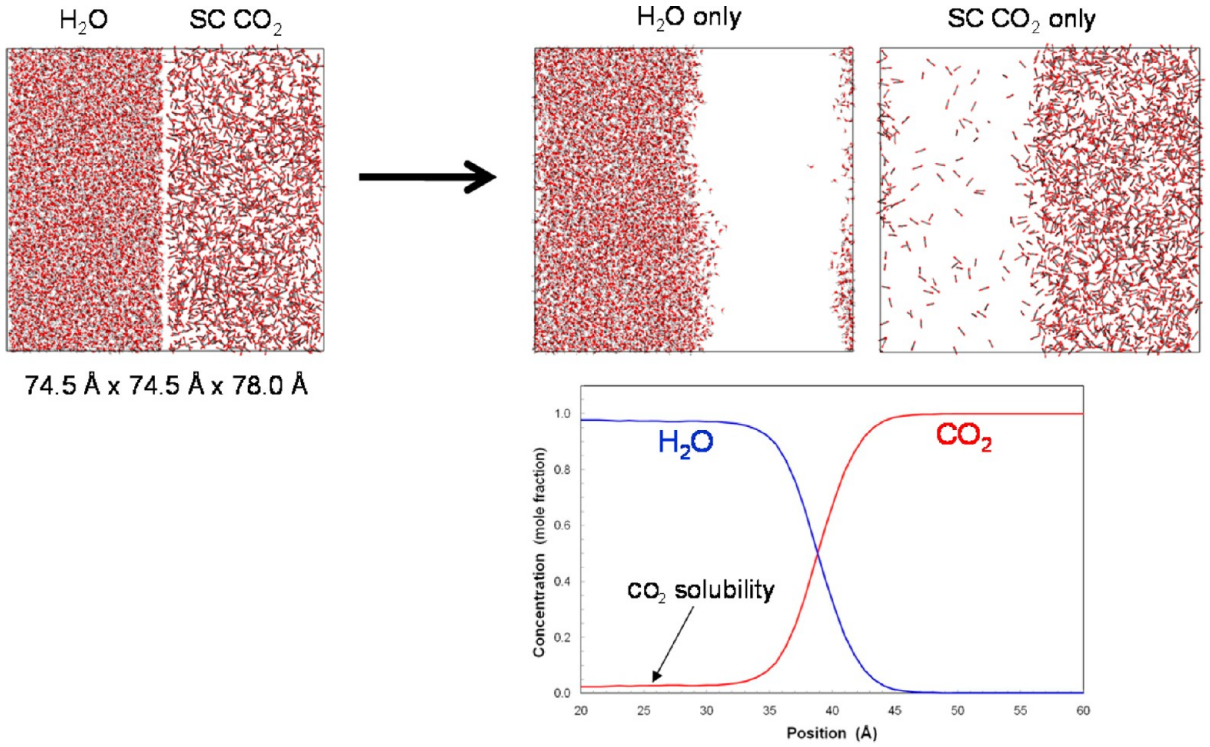

Figure 4. Initial configuration (left) and after 500 ps (right) of MD simulation cell showing water–supercritical CO_2 interface at 350 K and 20 MPa. Concentration variation for both components across the interface exhibit diffusional profile with finite solubility of CO_2 in water phase indicated.

dx.doi.org/10.1021/es301608c | Environ. Sci. Technol. 2013, 47, 87–94

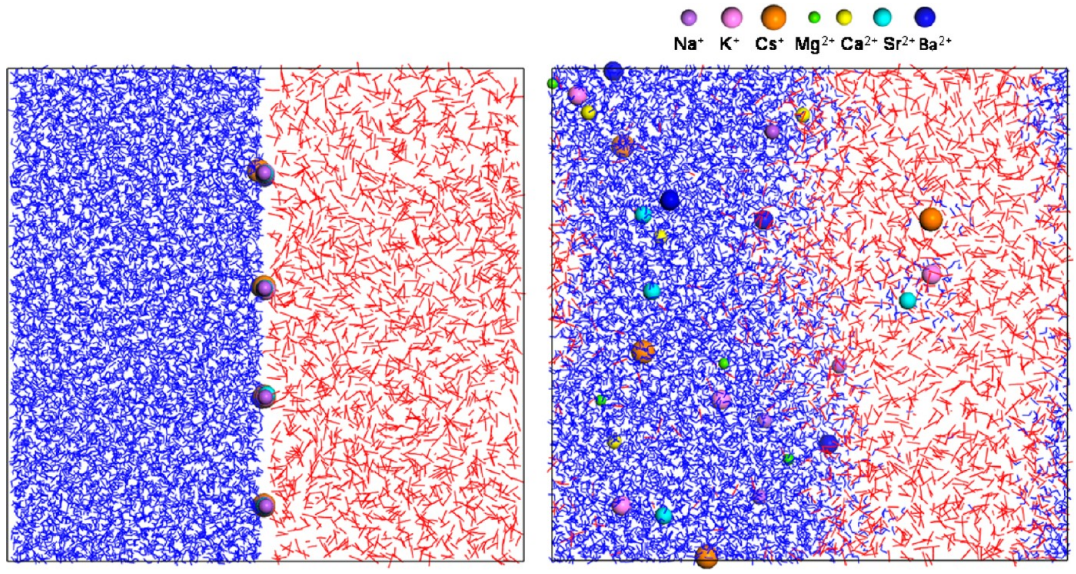

Figure 5. Initial configuration (left) and after 500 ps (right) of MD simulation cell of water−supercritical CO_2 system at 350 K and 20 MPa showing various cations near the CO_2 (red)−H_2O (blue) interface.

of cation species at the water−supercritical CO_2 interface. Molecular configurations for the initial simulation cell and after 0.5 ns of MD simulation for cation partitioning at the water−CO_2 interface are presented in Figure 5. In general, the MD results indicate the strong affinity of cations to partition into the aqueous phase with most of the alkali and alkaline earth cations fully solvated by water molecules. However, several cations exist in the CO_2 phase but are either partially (K^+ and Cs^+) or fully coordinated (Sr^{2+}) by water molecules (see Abstract graphic). The partial solvation of the alkali cations is consistent with the results of our analysis of solvation energies (Figure 3) where the larger monovalent cations prefer the aqueous phase but the energy difference for solvation by CO_2 phase is only about 10−20 kcal/mol. Therefore, it is not unexpected to have both water and CO_2 molecules comprising the first solvation sphere. In contrast, the occurrence of divalent Sr^{2+} in the CO_2 phase is surprising especially with a solvation energy difference of approximately 160 kcal/mol between solvents. In this MD simulation example, however, Sr^{2+} remains fully hydrated and the cation−water complex diffuses across the interface to exist completely within the CO_2 phase. Further calculations would be required to calculate the solvation of hydrated ions in a CO_2 solvent. Assuming stability, the hydrated cations (partial or fully) could contribute to an increase in water solubility in supercritical CO_2 fluids.

As in the pure water−CO_2 simulation, CO_2 molecules diffuse across the interface and into the aqueous phase but are typically not associated with the relatively high concentration of cations. In general, these results and more advanced molecular simulations of brine−supercritical CO_2 systems provide a novel approach for evaluating densities, solubilities, and related properties of complex natural systems that may not be easily determined through experimental means.

Implications. Molecular dynamics simulations with a flexible CO_2 force field have been used to derive structural and thermodynamic properties associated with the solvation of alkali and alkaline earth cations in CO_2 liquid. Interfaces between water and supercritical CO_2 with and without cations are simulated to demonstrate the utility of large-scale MD simulations for evaluating the evolution of fluid interfaces and the partitioning of cations. The solubility of supercritical CO_2 in H_2O at 350 K and 20 MPa is successfully predicted by combining flexible CO_2 and H_2O force fields.

As a first approximation in field-scale multiphase flow codes used to simulate various CO_2 sequestration scenarios, metal cations are assumed not to partition into nonpolar solvents such as supercritical CO_2.[14] However, these preliminary molecular simulations suggest that the difference in energy for alkali metal solvation in liquid water and CO_2 is relatively small (<40 kcal/mol). This difference decreases with increasing ionic radii, and in the large-scale interfacial simulations, the two larger monovalent cations, Cs^+ and K^+, that have nearly equivalent solvation energies in both solvents, do indeed partition between CO_2 and H_2O. In addition, in supercritical CO_2, the first solvation shell for both cations includes both CO_2 and H_2O molecules.

In contrast, the solvation energies for the divalent alkaline earth metal cations in CO_2 are much smaller than in water, suggesting that they are less likely to partition into supercritical CO_2 than the alkali metals. However, in our simulations, a Sr^{2+} cation partitions into the CO_2 solvent with a complete water solvation shell. This suggests that divalent and higher-charged metal cations may partition into supercritical CO_2 with hydration shells that buffer their charge.

These results imply that the metals in saline brines under reservoir conditions may partition into supercritical CO_2 and increase the concentration of water in this phase. Metal partitioning into the supercritical phase may influence chemical reactions such as the dissolution of primary minerals, precipitation of secondary phases, and the interaction between the two fluid phases. These simulations suggest that further classical molecular dynamics simulations should be performed to investigate the interaction of more realistic brine compositions with supercritical CO_2 over a range of geological repository conditions to evaluate the potential extent and impact of metal-partitioning into the supercritical phase.

dx.doi.org/10.1021/es301608c | *Environ. Sci. Technol.* 2013, 47, 87−94

AUTHOR INFORMATION

Corresponding Author

*Phone: 505-284-4357; fax: 505-844-7354; email: ljcrisc@sandia.gov.

Notes

The authors declare no competing financial interest.

ACKNOWLEDGMENTS

This work was funded in part by the Center for Frontiers of Subsurface Energy Security, an Energy Frontier Research Center funded by the U.S. Department of Energy, Office of Science, Office of Basic Energy Sciences under Award DE-SC-0001114. Sandia National Laboratories is a multiprogram laboratory operated by Sandia Corporation, a wholly owned subsidiary of Lockheed Martin Corporation, for the U.S. Department of Energy's National Nuclear Security Administration under Contract DE-AC04-94AL85000.

REFERENCES

(1) Dodds, W. S.; Stutzman, L. F.; Sollami, B. J. Carbon dioxide solubiltiy in water. *Ind. Eng. Chem. Res.* **1956**, *1*, 92−95.

(2) Takenouchi, S.; Kennedy, G. C. The binary system H_2O-CO_2 at high temperatures and pressures. *Am. J. Sci.* **1964**, *262* (9), 1055−1074.

(3) Takenouchi, S.; Kennedy, G. C. The solubility of carbon dioxide in NaCl solutions at high temperatures and pressures. *Am. J. Sci.* **1965**, *263* (5), 445−454.

(4) Ellis, A. J. The solubility of carbon dioxide in water at high temperatures. *Am. J. Sci.* **1959**, *257*, 217−234.

(5) Ellis, A. J.; Golding, R. M. The solubility of carbon dioxide above 100C in water and in sodium chloride solutions. *Am. J. Sci.* **1963**, *261*, 47−60.

(6) Malinin, S. D.; Savelyeva, N. I. The solubililty of CO_2 in NaCl and $CaCl_2$ solutions at 25, 50, and 75 degrees under elevated CO_2 pressures. *Geochem. Int.* **1972**, *6*, 410−418.

(7) Malinin, S. D.; Kurovskaya, N. A. Solubility of CO_2 in chloride solutions at elevated temperatures and CO_2 pressures. *Geochem. Int.* **1975**, *2*, 199−201.

(8) Cole, D. R.; Chialvo, A. A.; Rother, G.; Vlcek, L.; Cummings, P. T. Supercritical fluid behavior at nanoscale interfaces: Implications for CO_2 sequestration in geologic formations. *Philos. Mag.* **2010**, *90* (17−18), 2339−2363.

(9) Giesting, P.; Guggenheim, S.; Koster van Groos, A. F.; Busch, A. Interaction of carbon dioxide with Na-exchanged montmorillonite at pressures to 640 bar: Implications for CO_2 sequestration. *Int. J. Greenhouse Gas Control* **2012**, *8*, 73−81.

(10) Kharaka, Y. K.; Cole, D. R. Geochemistry of geologic sequestration of carbon dioxide. In *Frontiers in Geochemistry: Contribution of Geochemistry to the Study of the Earth*; Harmon, R. S., Parker, A., Eds.; Blackwell Publishing, 2011.

(11) Spycher, N.; Pruess, K.; Ennis-King, J. CO_2-H_2O mixtures in the geological sequestration of CO_2: I. Assessment and calculation of mutual solubilities from 12 to 100°C and up to 600 bar. *Geochim. Cosmochim. Acta* **2003**, *67* (16), 3015−3031.

(12) Spycher, N.; Pruess, K. CO_2-H_2O mixtures in the geological sequestration of CO_2: II. Partitioning in chloride brines at 12−100°C and up to 600 bar. *Geochim. Cosmochim. Acta* **2005**, *69* (13), 3309−3320.

(13) Rempel, K. U.; Liebscher, A.; Heinrich, W.; Schettler, G. An experimental investigation of trace element dissolution in carbon dioxide: Applications to the geological storage of CO_2. *Chem. Geol.* **2011**, *289*, 224−234.

(14) Wigand, M.; Carey, J. W.; Schutta, H.; Spangenberg, E.; Erzinger, J. Geochemical effects of CO_2 sequestration in sandstones under simulated in situ conditions of deep saline aquifers. *Appl. Geochem.* **2008**, *23* (9), 2735−2745.

(15) Laintz, K. E.; Wai, C. M.; Yonker, C. R.; Smith, R. D. Extraction of metal ions from liquid and solid materials by supercritical carbon dioxide. *Anal. Chem.* **1992**, *64* (22), 2875−2878.

(16) Cygan, R. T.; Romanov, V. N.; Myshakin, E. M. Molecular simulation of carbon dioxide capture by montmorillonite using an accurate and flexible force field. *J. Phys. Chem. C* **2012**, *116* (24), 13079−13091.

(17) Zhu, A. M.; Zhang, X. B.; Liu, Q. L.; Zhang, Q. G. A fully flexible potential model for carbon dioxide. *Chin. J. Chem. Eng.* **2009**, *17* (2), 268−272.

(18) Harris, J. G.; Yung, K. H. Carbon dioxide's liquid-vapor coexistence curve and critical properties as predicted by a simple molecular model. *J. Phys. Chem.* **1995**, *99* (31), 12021−12024.

(19) Cygan, R. T.; Liang, J.-J.; Kalinichev, A. G. Molecular models of hydroxide, oxyhydroxide, and clay phases and the development of a general force field. *J. Phys. Chem. B* **2004**, *108* (4), 1255−1266.

(20) Allen, M. P.; Tildesley, D. J. *Computer Simulation of Liquids*; Oxford University Press: Oxford, 1987; p 385.

(21) Halgren, T. A. Representation of van der Waals (vdW) interactions in molecular mechanics force fields: Potential form, combination rules, and vdw parameters. *J. Am. Chem. Soc.* **1992**, *114* (20), 7827−7843.

(22) Accelrys. *Materials Studio, Release* 5.5; Accelrys Software Inc.: San Diego, CA, 2010.

(23) Nosé, S. A molecular dynamics method for simulations in the canonical ensemble. *Mol. Phys.* **1984**, *52* (2), 255−268.

(24) Franks, F. *Aqueous Solutions of Simple Electrolytes*; Springer: New York, 1973; Vol. *3*, p 472.

(25) Smith, D. E.; Dang, L. X. Computer simulations of NaCl association in polarizable water. *J. Chem. Phys.* **1994**, *100*, 3757−3766.

(26) Goodisman, J. A model for the surface of molten salt. II. Electroneutrality and parameter changes. *J. Chem. Phys.* **1978**, *69* (12), 5340−5348.

(27) Berendsen, H. J. C.; Postma, J. P. M.; van Gunsteren, W. F.; Hermans, J. Interaction models for water in relation to protein hydration. In *Intermolecular Forces*; Pullman, B., Ed.; D. Reidel, 1981; pp 331−342.

(28) Teleman, O.; Jonsson, B.; Engstrom, S. A molecular dynamics simulation of a water model with intramolecular degrees of freedom. *Mol. Phys.* **1987**, *60* (1), 193−203.

(29) Piquemal, J.-P.; Perera, L.; Cisneros, G. A.; Ren, P.; Pedersen, L. G.; Darden, T. A. Towards accurate solvation dynamics of divalent cations in water using the polarizable amoeba force field: From energetics to structure. *J. Chem. Phys.* **2006**, *125*, 054511.

(30) Whitfield, T. W.; Varma, S.; Harder, E.; Lamoureux, G.; Rempe, S. B.; Roux, B. Theoretical study of aqueous solvation of K^+ comparing ab initio, polarizable, and fixed-charge models. *J. Chem. Theory Comput.* **2007**, *3*, 2068−2082.

(31) Ishii, R.; Okazaki, S.; Okada, I.; Furusaka, M.; Watanabe, N.; Misawa, M.; Fukunaga, T. Density dependence of structure of supercritical carbon dioxide along an isotherm. *J. Chem. Phys.* **1996**, *105* (16), 7011−7021.

(32) Ohtaki, H.; Radnai, T. Structure and dynamics of hydrated ions. *Chem. Rev.* **1993**, *93*, 1157−1204.

(33) D'Angelo, P.; Petit, P. E.; Pavel, N. V. Double-electron excitation channels at the Ca^{2+} K-edge of hydrated calcium ion. *J. Phys. Chem. B* **2004**, *108* (31), 11857−11865.

(34) Jalilehvand, F.; Spangberg, D.; Lindqvist-Reis, P.; Hermansson, K.; Persson, I.; Sandstrom, M. Hydration of the calcium ion. An EXAFS, large-angle X-ray scattering, and molecular dynamics simulation study. *J. Am. Chem. Soc.* **2001**, *123* (3), 431−441.

(35) Sandstrom, M.; Persson, I.; Jalilehvand, F.; Lindquist-Reis, P.; Spangberg, D.; Hermansson, K. Hydration of some large and highly charged metal ions. *J. Synchrotron Radiat.* **2001**, *8*, 657−659.

(36) O'Day, P. A.; Newville, M.; Neuhoff, P. S.; Sahai, N.; Carroll, S. A. X-ray absorption spectroscopy of strontium(II) coordination: I. Static and thermal disorder in crystalline, hydrated, and precipitated solids and in aqueous solution. *J. Colloid Interface Sci.* **2000**, *222* (2), 184−197.

(37) Persson, I.; Sandstrom, M.; Yokoyama, H.; Chaudhry, M. Structure of the solvated strontium and barium ions in aqueous, dimethyl sulfoxide and pyridine solution, and crystal structure of strontium and barium hydroxide octahydrate. *Z. Naturforsch., A: Phys. Sci.* **1995**, *50* (1), 21−37.
(38) Larentzos, J. P.; Criscenti, L. J. A molecular dynamics study of alkaline earth metal-chloride complexation in aqueous solution. *J. Phys. Chem. B* **2008**, *112* (45), 14243−14250.
(39) Vlcek, L.; Chialvo, A. A.; Cole, D. R. Optimized unlike-pair interactions for water-cabon dioxide mixtures described by the SPC/E and EPM2 models. *J. Phys. Chem. B* **2011**, *115* (27), 8775−8784.
(40) Åqvist, J. Ion-water interaction potentials derived from free energy perturbation simulations. *J. Phys. Chem.* **1990**, *94*, 8021−8024.
(41) Koneshan, S.; Rasaiah, J. C.; Lynden-Bell, R. M.; Lee, S. H. Solvent structure, dynamics, and ion mobility in aqueous solutions at 25 °C. *J. Phys. Chem. B* **1998**, *102* (21), 4193−4204.
(42) Smith, D. E.; Dang, L. X. Computer simulations of cesium-water clusters: Do ion-water clusters form gas-phase clathrates? *J. Chem. Phys.* **1994**, *101*, 7873−7881.